Electron Transmission Through Thin Metal Sections with Application to Self-Recovery in Cold Worked Aluminum

By R. D. HEIDENREICH

Features of the dynamical or wave mechanical theory of electron diffraction pertinent to the interpretation of electron images of crystalline materials are briefly discussed. It is shown that the type of image obtained depends upon the local bending of the crystal, the coherent crystal size and the state of internal strain. The absence of extinction contours seen in annealed aluminum is an indication of the presence of internal strains.

New data concerning the effect of temperature on the polygon or domain size in cold worked aluminum is presented. These data indicate that self recovery occurs rapidly at temperatures as low as −196°C leading to the conclusion that the process must have a low activation energy. The mechanism by which dislocations leave the slip bands and redistribute and annihilate themselves during recovery is obscure.

Introduction

DIRECT experimental evidence for the wave nature of the electron first demonstrated by Davisson and Germer was based on a property unique to wave phenomena; namely, interference or diffraction. The ability of a regular or periodic array of atoms to diffract electrons (just as a ruled grating diffracts light) has led to the construction of quite general theories of the behavior of matter, the band theory of solids being a notable example. The forbidden energy zones in a crystal are simply a result of diffraction of the valence electrons by the periodic structure. On the other hand, the results of straight forward diffraction experiments are a consequence of the zone or band structure of the crystal thus illustrating an interesting closure or completion of the cycle.

This paper is concerned with the interpretation of electron interference phenomena occurring in thin metal sections particularly as it pertains to structural changes accompanying plastic deformation. Diffraction effects are observed not only in the usual electron diffraction methods but in electron microscope images as well. The chief difference is that in the former the diffracted rays are of primary interest while in the latter the regions of the crystal in which diffraction occurs are imaged with the diffracted beams removed by the objective aperture. Electron microscope images of crystalline materials thus offer a high resolution method of studying variations in diffracting power. This information can then be interpreted in terms of structural features.

The structural changes accompanying plastic deformation of metals are of great interest and can be profitably investigated by electron interference

techniques. In particular the loss of work hardening in pure metals by the process of self-recovery is well suited to study using the electron microscope and thin sections, as will be seen. In a previous paper[1] the technique of preparing thin aluminum sections and the interpretation of the diffraction features were discussed in detail. The dynamical theory of electron diffraction has been applied to this particular problem and also extended to more general cases.[2] It was shown[1] that, immediately after cold working, high purity aluminum exhibits a sub-grain or domain structure of the order of 1–2 microms in size. These domains are slightly misoriented and become visible in electron images through small variations in diffracted intensity in passing from one domain to the next. The domains have been identified with self-recovery following plastic deformation but their properties and origin have not been investigated in detail. The experiments to be described here include the effect of electron bombardment, and the effect of temperature on the size of the domains.

It should be pointed out that the term "recovery domains" has been applied by the writer to the sub-grains or units appearing in cold worked aluminum. It appears now that the recovery domains are an early stage of the process of "polygonization" commonly used in the literature. Polygonization was first applied to the formation of larger blocks or polygons in bent crystals that were annealed at an elevated temperature. The polygons were made visible in a light microscope by the use of an etchant which produced etch pits in the polygon boundaries.[3] Either term, polygonization or recovery domains, would be suitable although the latter is more specific as to the process involved and will be used in this paper.

Dynamical Theory Applied to Electron Images

The wave mechanical or dynamical theory of electron diffraction is essential to the interpretation of electron images of crystals. The kinematic theory, a simpler approximation, is not adequate. Consequently, it is advisable at this point to review briefly the salient features of the dynamical theory as applied to electron images.*

Suppose a polycrystalline film (such as a thin metal section) is mounted in the conjugate focal plane of the objective lens of an electron microscope as depicted in Fig. 1. Let the incident electron beam be taken as monochromatic and plane-parallel. Regions of the specimen film oriented such that a set of net planes satisfies the Bragg condition $n\lambda = 2d \sin \theta$ will

[1] R. D. Heidenreich, *Jl. App. Phys. 20*, 993 (1949).
[2] R. D. Heidenreich, *Phys. Rev. 77*, 271 (1950).
[3] P. Lacombe and L. Beaujard, "Report of a Conference on Strength of Solids," p. 91 (Physical Society, London, 1948).
* Detailed treatments are given in references 1 and 2.

diffract the incident beam of wave length λ through an angle 2θ. d is the interplanar spacing. The numerical aperture of the electron lens is such that in general $2\theta > \alpha_{ob}$ with the result that the diffracted beams are removed from the optical system and not focused in the image plane. In Fig. 1, crystals 1 and 3 are suitably oriented to diffract and so will appear dark in the final image since electrons have been removed from these regions by Bragg reflection. The calculations of the intensities for this case (the Laue case) were first made by Bethe.[4] A similar treatment[1,2] employing the zone theory of crystals can be given which yields the same final results. The procedure consists in solving the Schrödinger equation for an electron moving in the

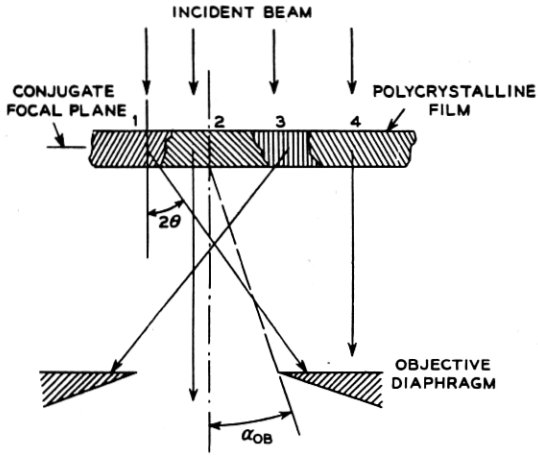

Fig. 1—Diffraction of electrons outside objective aperture by suitably oriented crystals in polycrystalline film. Crystals 1 and 3 would appear dark in final image.

periodic potential inside the crystal and then fitting the solutions so obtained to the plane wave solution found for the vacuum incident and diffracted waves. The first result of the solution inside the crystal is that the total energy of the electron, E, is not a continuous function of the wave number K ($|K| = \frac{2\pi}{\lambda}$) as it is in field-free space, but exhibits discontinuities as illustrated in Fig. 2. These discontinuities occur whenever the Bragg or Laue condition is satisfied; i.e., if g is a vector of the reciprocal lattice, then discontinuities in the E vs K curve occur when $|K| = |K + 2\pi g|$ which is equivalent to the Bragg formula. The magnitude of the energy

[4] H. A. Bethe, *Ann. d. Physik 87*, 55 (1928). This treatment was intended to explain the results of Davisson and Germer which were published about a year before. Had Bethe examined the behavior of the total energy in his solution of the Schrödinger equation he would have discovered the band theory of crystals.

gap[5] is $\Delta E = 2|Vg|$ where Vg is the Fourier coefficient of potential. The discontinuities in energy are the Brillouin zone boundaries and form a family of polyhedra in reciprocal or K space. For example, a simple square lattice gives rise to a square reciprocal lattice as seen in Fig. 3. One reciprocal lattice point is taken as the origin, 0, and the remainder of the lattice is generated by the vector g where $|g| = \frac{1}{a}$, the reciprocal of the cell constant of the original, direct lattice. The Brillouin zone boundaries are the perpendicular bisectors of the reciprocal lattice vectors[6] and define the series of zones shown in Fig. 3a. Whenever the incident electron wave vector, K,

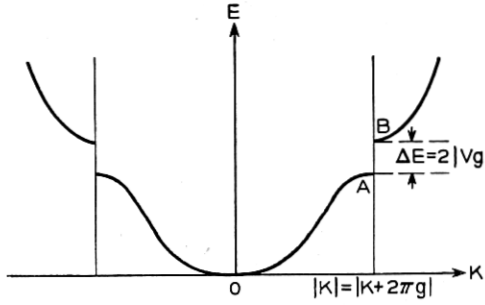

Fig. 2—Plot of energy, E, vs. wave number $|K|$, along K vector showing discontinuity when $|K| = |K + 2\pi g|$ or when Bragg condition is realized.

terminates on a Brillouin zone boundary, a diffracted wave is possible. However, when the boundary conditions at the surfaces of the crystal are applied, it turns out that for a fixed total energy, E, there are two incident crystal wave vectors K_0^0 and K_1^1 which must be considered. Consequently there are also two diffracted wave vectors K_g^0 and K_g^1 with $K_g^0 = K_0^0 + 2\pi g$ and $K_g^1 = K_0^1 + 2\pi g$ as shown in Fig. 3b. K_g^1 and K_g^0 are related by a beat wave vector ΔK or $K_g^1 = K_g^0 + \Delta K$. The net result is two waves of slightly different wave length traveling nearly parallel which may undergo interference. This beating of the diffracted waves makes itself known by passing the energy back and forth between the incident and diffracted beams. This is the motivation for the name "dynamical" theory.

The intensity of a diffracted beam for the case when the incident wave vector terminates near a Brillouin zone boundary but far from an edge or corner is found to be[1]:

[5] This treatment is the case of loose binding which is applicable for fast electrons. It turns out that for the valence electrons in a crystal, this approximation is not very good and that the value $\Delta E = 2|Vg|$ is not correct.

[6] L. Brillouin, "Wave Propagation in Periodic Structures," McGraw-Hill Book Company, Inc., New York (1946).

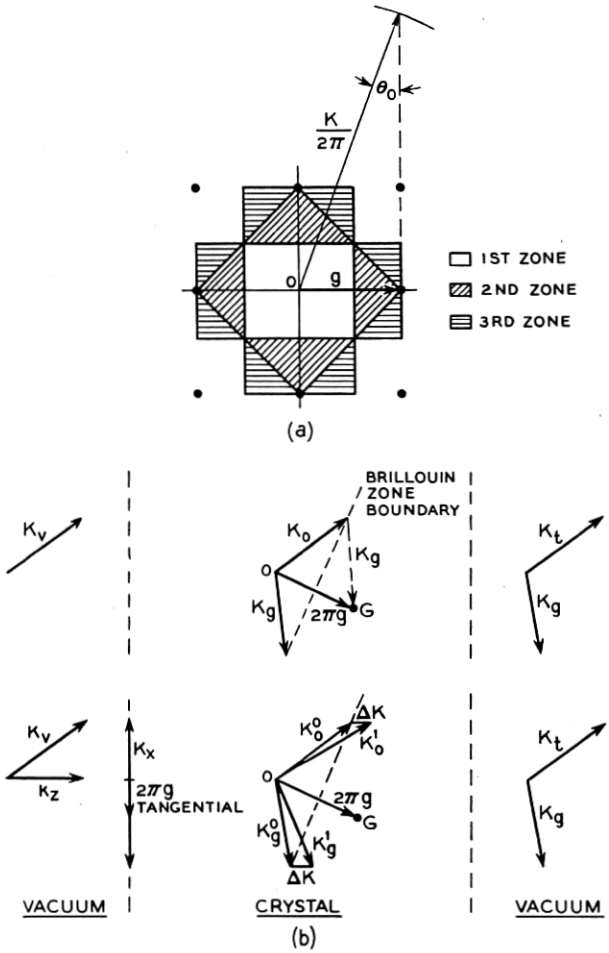

Fig. 3—(a). First three Brillouin zones for a simple square lattice. In an actual case, $|g|$ is of the order of $0.5A^{-1}$ and $\left|\frac{K}{2\pi}\right|$ about $19A^{-1}$.

(b). Relation among wave vectors in reciprocal space for the kinematic and for the dynamical theories. The wave vectors must satisfy the Bragg condition and the boundary conditions at the crystal faces. The dynamical theory introduces the beat wave vector ΔK. K_v is the vacuum incident wave vector.

$$Ig = \frac{|Vg|^2}{\left(\frac{\Delta g}{2}\right)^2 + |Vg|^2} \sin^2 \tfrac{1}{2}\Delta Kz \qquad (1)$$

where Vg = Fourier coefficient of potential

Δg = deviation from the Laue condition in volts

$= 2E\Delta\theta \sin 2\theta_0$

E = total energy of incident electrons in volts

θ_0 = Bragg angle

$\Delta\theta$ = angular deviation from Bragg condition

ΔK = beat wave vector

$$= \frac{2}{\lambda E}\left(\left(\frac{\Delta g}{2}\right)^2 + |Vg|^2\right)^{\frac{1}{2}}$$

z = penetration measured normal to surface of crystal

D = thickness of crystal

It is evident from equation (1) that the intensity of the diffracted beam is periodic with penetration in the crystal and with the deviation, Δg. This dependence of intensity upon thickness and deviation accounts for most of the image detail seen in electron micrographs of thin crystalline sections. Inelastic scattering and crystal imperfections are neglected in the derivation of equation (1).

Experience with thin sections of pure aluminum has indicated that it is nearly impossible to prepare and handle them without introducing some bending or rumpling of the thin area. This bending in conjunction with thickness variations gives rise to the major features of the electron images in the form of intensity maxima and minima called "extinction contours." Those arising through bending of the section are of chief interest in the uniform area where thickness changes are very gradual. The extinction contours are determined by the maxima of equation (1) or where $\Delta KD = n\pi$ to give

$$\Delta g = \pm\left(\frac{(n\lambda E)^2}{D} - 4|Vg|^2\right)^{\frac{1}{2}} \qquad n = 1, 3, 5, \ldots \tag{2}$$

Equation (2) predicts that for a bent crystal offering a continuous range of Δg a series of intensity maxima or fringes will be observed. In an electron image of a bent crystal the spacing of the fringes is the only quantity which can be measured other than relative intensity. The central fringe corresponds to $\Delta g = 0$ with subsidiary maxima occurring at a distance s from the central fringe given by[1]

$$s = \left(R + \frac{D}{2}\right)\frac{\Delta g}{2E \sin 2\theta_o} \tag{3}$$

where R is the radius of curvature of the bending.

If two crystallites in a thin section differ only slightly in orientation and the bending is favorable, then a series of fringes will occur in the two crystals with a displacement at the boundary as sketched in Fig. 4.

The displacement l is related to the orientation difference $\Delta\alpha$ and the

radius of curvature R by

$$\Delta\alpha = \frac{l}{R} \tag{4}$$

If the situation is such that R can be determined from equation (3), then the misorientation $\Delta\alpha$ can be calculated from (4). This combination of circumstances is at present one of chance and does not occur frequently in images of thin sections. An example will be shown.

The image contrast between adjacent regions of a thin metal section composed of small misoriented domains as depicted in Fig. 1 is determined by the rocking curve of equation (1). This is simply a plot of the intensity given by (1) against Δg or $\Delta\theta$. As an example, a rocking curve for the (200)

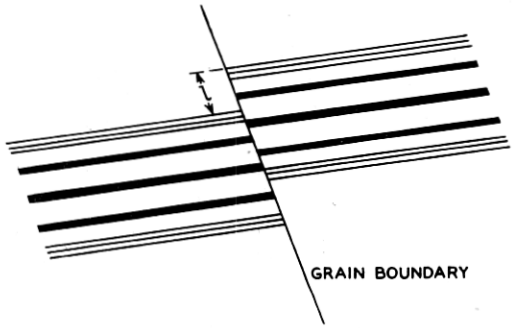

Fig. 4—Displacement (l) at a grain boundary of extinction contours due to bending as predicted by equations (3) and (4).

reflection of aluminum is shown in Fig. 5. The Fourier coefficient Vg is computed from the relation.*

$$V_{hkl} = 300\frac{ed^2_{hkl}}{\pi\Omega}\sum_j (Z_j - f_j)e^{2\pi i}\,(hu_j + kv_j + lw_j) \text{ volts} \tag{5}$$

with e = charge on the electron = 4.80×10^{-10} *esu*
Ω = volume of the unit cell = 70.4 A^3 for aluminum
d_{hkl} = interplanar spacing
Z_j = atomic number of atom species j
f_j = atom form factor
(u_j, v_j, w_j) = atomic coordinates of atom species j

For aluminum, $V_{(200)} = 5.13$ volts. Using 50KV electrons: $E = 5 \times 10^4$, $\lambda = 0.055$A, $\sin 2\theta_0 = 0.0272$ radian and a reasonable value of $D = 250$A, the intensity can be computed from (1) as a function of Δg as shown in Fig. 5.

* Reference 1, Appendix I.

It will be realized that the detailed shapes and location of the maxima are quite sensitive to thickness and more often than not a calculation from the fringe spacings cannot be made with certainty. The limiting value of the fringe separation is found from (2) to be given by $\frac{d_{hkl}}{D}$ for large values of the integer n. The fringe pattern indicated in Fig. 4 is simply a rocking curve for the crystallites with a displacement due to their difference in orientation.

The absence of extinction contours from the electron image of a crystal may indicate that one or more of the following conditions exists:

(1) No bending or thickness changes.

(2) The thickness is sufficiently small that the argument of the $\sin^2$ in

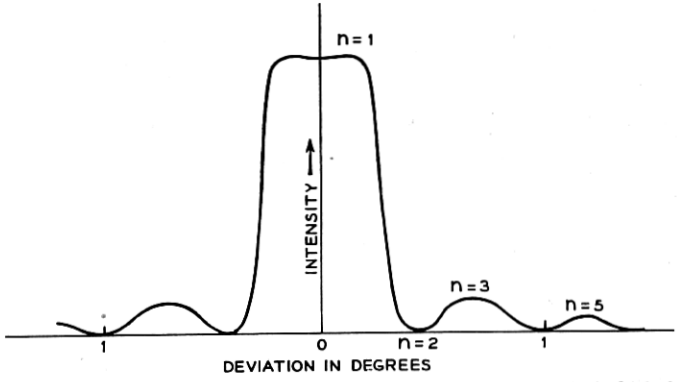

Fig. 5—(200) rocking curve calculated for an aluminum crystal 250A thick for 50KV electrons.

(1) can replace the sine function thus suppressing the periodic features; this can occur for D less than about 100A.

(3) The crystal is sufficiently distorted that the assumption of a periodic potential function in the Schrödinger equation is not valid.

Of these causes for the absence of extinction contours, the first is very unlikely as mentioned previously. The second is quite obvious since a section too thin to produce contours would give a very high transmitted intensity and would be immediately apparent. The third is the most likely reason and is thought to be the case in all the thin sections examined to date. This is particularly important here since crystals that have been subjected to plastic deformation are of primary interest. The incorporation of strains or lattice disortion into the potential function for the Schrödinger equation appears to be a formidable task and will not even be attempted. A more or less semi-quantitative approach to the effect of lattice distortion

can be had by considering the expression for the diffracted intensity (equation (1)). If dislocations are introduced into a crystal the effect is that of producing a mosaic or block structure[7] the units of which will scatter incoherently. If there are a sufficient number of dislocations to reduce the coherent penetration path z to a value z' such that $\Delta K z'$ is small, then equation (1) will become

$$Ig \simeq \frac{|V_g|^2}{\left(\frac{\Delta g}{2}\right)^2 + |V_g|^2} \tfrac{1}{4} (\Delta K z')^2 = \frac{\pi^2}{\lambda^2 E^2} |V_g|^2 (z')^2 \tag{6}$$

The important part in considering equation (6) is the disappearance of the periodic, dynamic term. If the model obtained by introducing dislocations into the crystal even roughly approximates the actual situation then it would be expected from equation (6) that the extinction contours will vanish. Actually, starting with a perfect crystal and adding dislocations, the dynamical effects will not be noticeably effected until the coherent penetration z' becomes much smaller than $\frac{\lambda E}{V_g}$. For 50 KV electrons in aluminum, z' would have to be something of the order of 150A or less before the dynamical effects would disappear. If the model is carried still further, it can be speculated that z' is the mean separation of dislocations in the crystal indicating that a distance of separation of the order of 150A is required to extinguish the extinction contours. This would correspond to a dislocation density of about 5×10^{11} lines/cm^2. This is admittedly a very crude approximation and, although the dislocation density is of the right order of magnitude, too much significance should not be attached to it. It does seem fairly safe to conclude that the extinction contours will disappear when the dislocation density reaches a high enough value. This fact in itself greatly broadens the interpretation of the electron micrographs to be presented.

Preparation of Thin Aluminum Sections

The details of the preparation of the thin sections used for electron microscopy have been published[1] and are not vital to the discussion. Suffice it to say that the sections are produced from 0.005″ sheet by an electropolishing technique using a special holder. The central portion of the metal disc is thinned down to several hundred Angstroms or less while maintaining a smooth surface. A rinsing procedure is necessary to prevent the formation of corrosion layers.

[7] R. D. Heidenreich and W. Shockley, Report of a Conference on Strength of Solids, p. 57 (Physical Society, London, 1948).

The metal used in all this work was 99.993% French aluminum rolled into 0.005″ sheet.

Recovery of Cold Worked Aluminum

Having briefly discussed the essential phenomena in interpreting electron images of crystals, the application of the thin section method to self-recovery in deformed aluminum can be demonstrated. This type of investigation is based to a considerable extent upon comparison of images of the metal

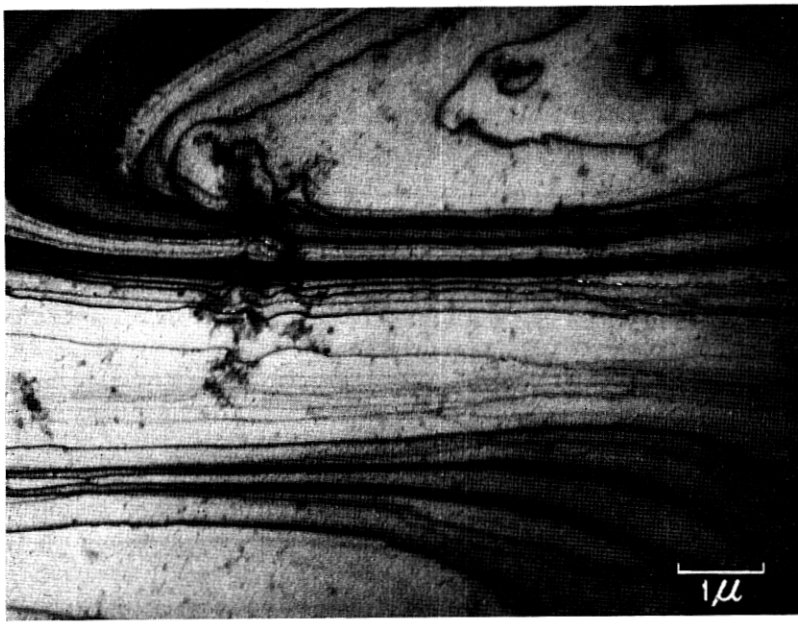

Fig. 6—Extinction contours due to rumpling in an annealed high purity (99.993) aluminum section.

under various conditions of anneal and plastic deformation. The standard state for comparison is a well annealed specimen in which the crystals are reasonably perfect. The bending or rumpling produces the extinction contour patterns quite unique to the annealed condition. The chief characteristics of the contours for an annealed crystal are their general continuity and extension over relatively large areas. Figure 6 illustrates a contour pattern with an unusually high density of lines obtained from an aluminum section annealed 30 min. at 335°C. The dark regions are those of electron deficiency.

At a grain boundary in an annealed section the contours end abruptly

as seen in Fig. 7a. Figure 7b illustrates a case in which the contour family can be identified on either side of a grain boundary with the displacement very much in evidence at the boundary. This situation was anticipated in Fig. 4.

Proof that the dark contour lines seen in Fig. 6 are due to diffraction from those regions was given in reference (1) where both the transmitted and diffracted beams were imaged in an electron shadow microscope. The usual transmission electron diffraction patterns from annealed sections generally exhibit an array of spots characteristic of a single crystal. Sometimes weak, broad Kikuchi lines are obtained but generally the bending of the section and the area of the incident electron beam are such as not to favor Kikuchi lines.

The effect of cold working on the images of the sections was studied by lightly pounding the center region of a $\frac{1}{8}''$ diameter disc (0.005″ thick) with a small, rounded and polished steel rod against an anvil. The disc was then electro-thinned and examined in the electron microscope. Originally it was hoped that further information regarding laminar slip[7] might be obtained in this manner. However, no details of slip have been observed in the cold worked sections, the general appearance being that seen in Fig. 8(a). Figure 8 was obtained from a section cold worked by pounding at room temperature and shows the recovery domains or early stage of polygonization.[8] These domains are not made visible by etching a polished surface and are observed only by electron transmission. The domains are slightly disoriented one with respect to the other and are made visible by the differences in diffracted intensity. Since the extinction contours are absent in Fig. 8a it is concluded that there is considerable internal strain in the domains as previously mentioned. Figure 8b is a transmission electron diffraction pattern of this section and shows arced rings made up of discrete spots. It is concluded that each spot on an arc corresponds to a domain. Insufficient domains are included in the primary beam to produce continuous rings. The electron diffraction pattern of Fig. 8b is very similar to microbeam x-ray patterns published by Kellar[9] et al and the domain size of about 2μ from the electron micrographs is in excellent agreement with the results of Kellar for pure aluminum.

That domains sufficiently free of strain to yield extinction contours can be obtained is illustrated in Fig. 9. Figure 9a is from a section prepared 36 hours after a block of the high purity aluminum had been rolled to 0.005″ sheet with some annealing between passes. The contours are very much in

[8] Recovery domains are not found in aluminum deformed by simple extension. Apparently inhomogeneous strain is necessary. Extinction contours are observed in specimens deformed in tension but the slip bands are not in evidence.

[9] J. N. Kellar, P. H. Hirsch and J. S. Thorp, *Nature 165*, 554 (1950).

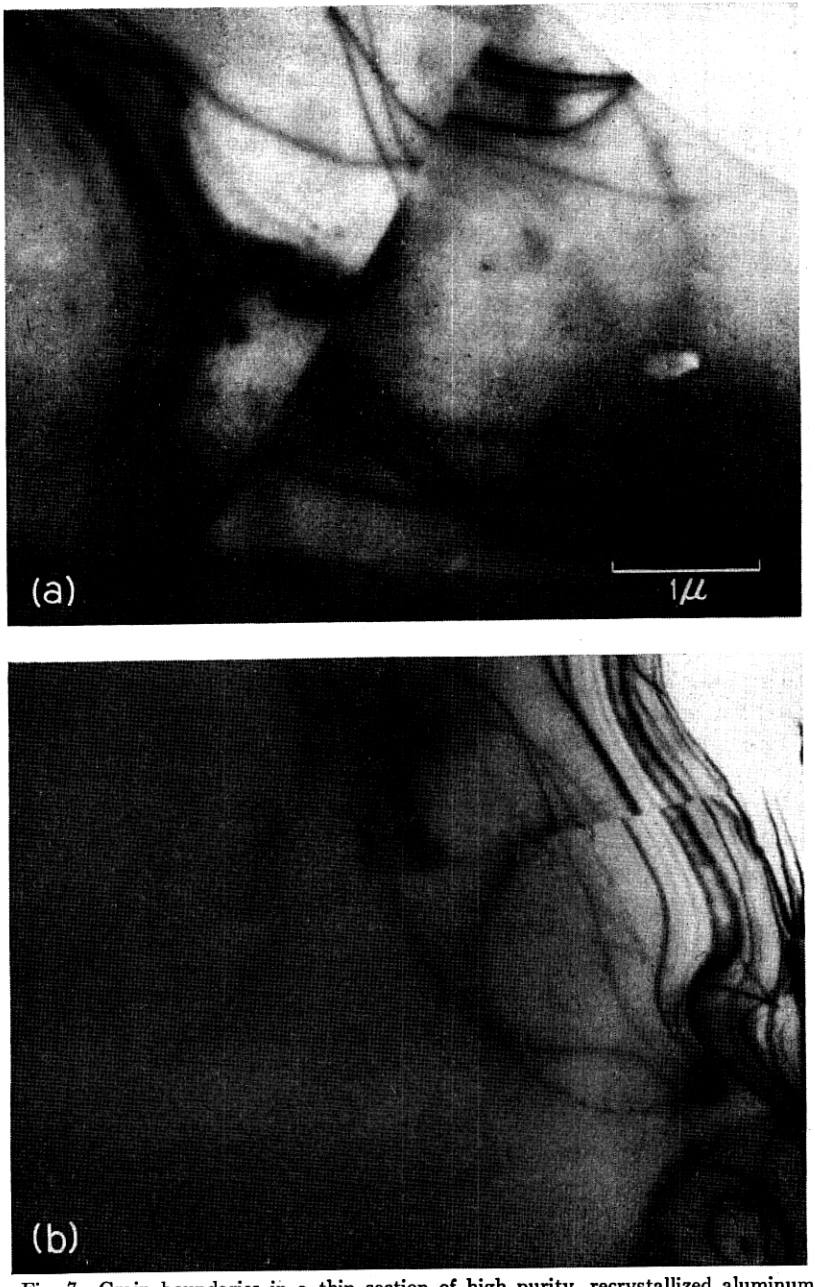

Fig. 7—Grain boundaries in a thin section of high purity, recrystallized aluminum. The displacement of a family of contours at the boundary is evident in (b).

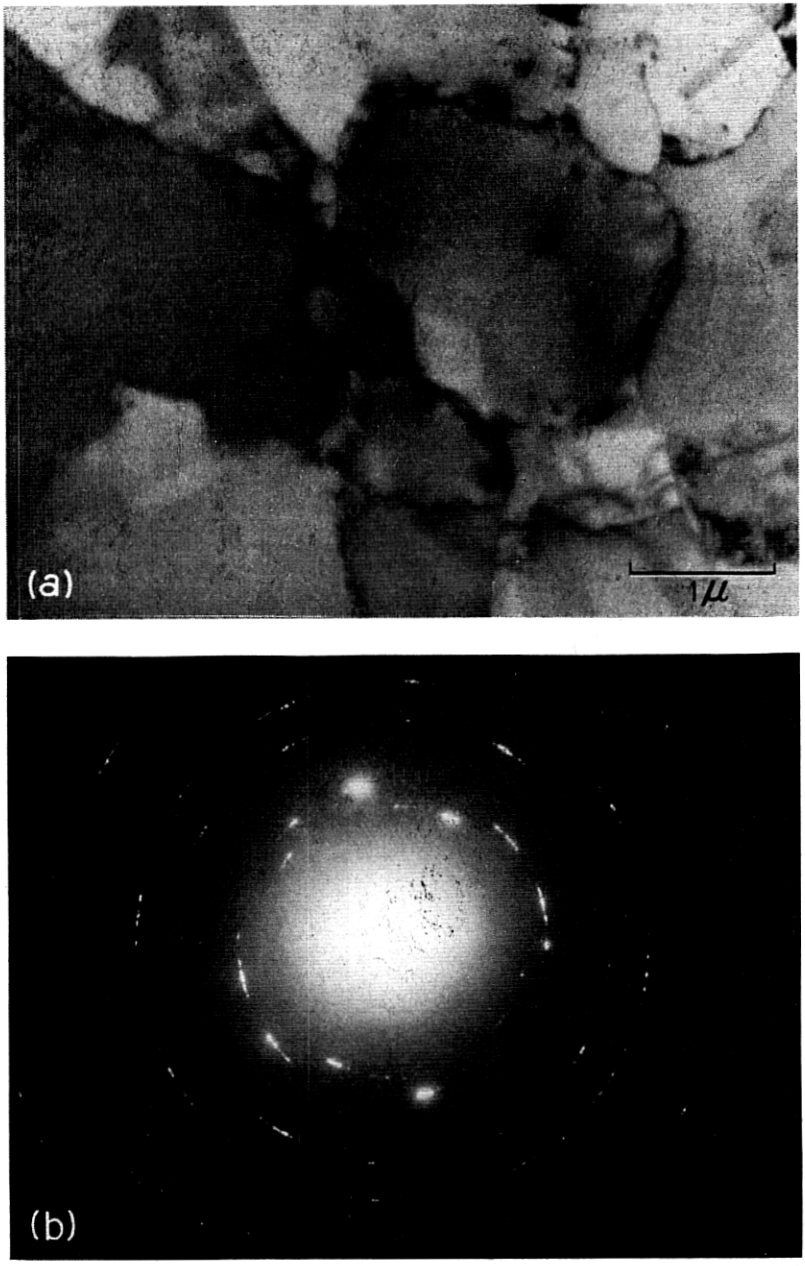

Fig. 8—Thin section of high purity aluminum cold worked by pounding. The recovery domains are evident in (a). (b) is an ordinary electron diffraction pattern (transmission) of the section and shows the discrete spots on the arced rings.

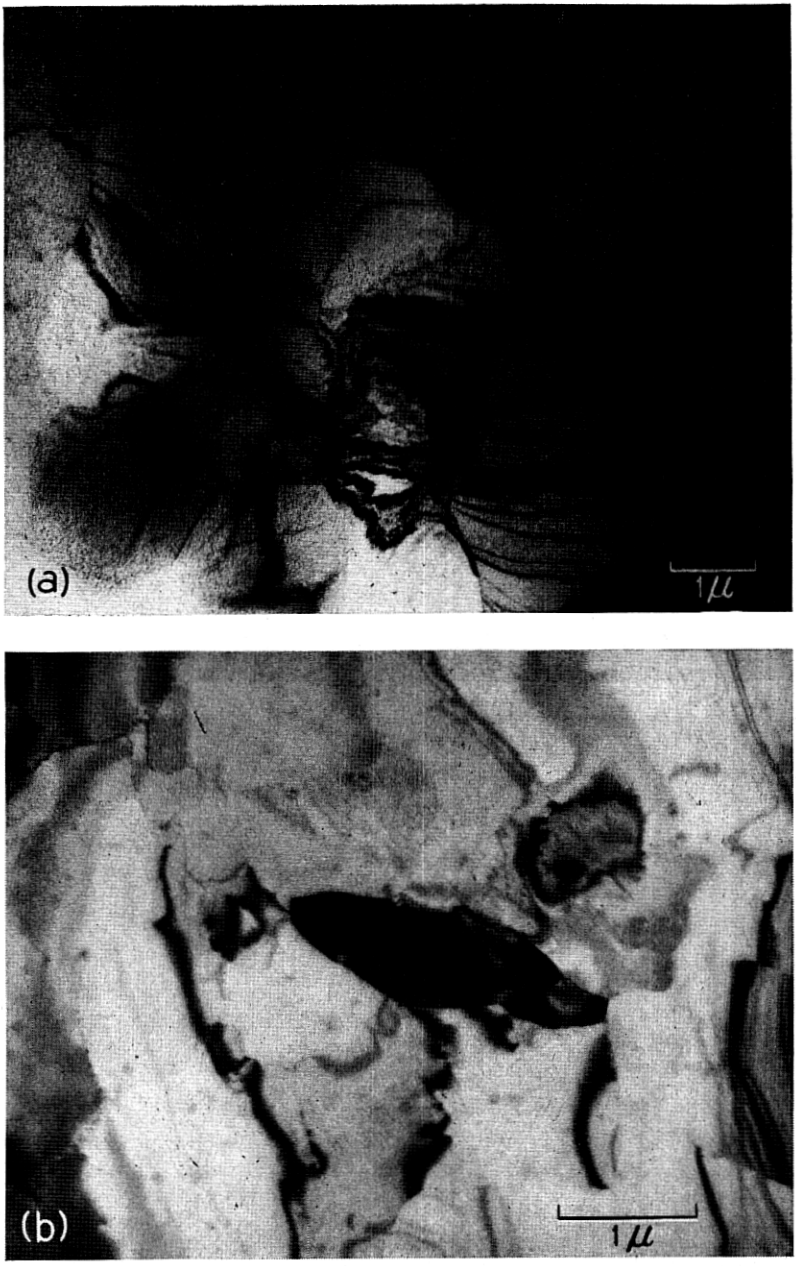

Fig. 9—Recovery domains in rolled, high purity aluminum annealed between passes through the rolls.

(a). 36 hrs. after rolling showing extinction contours in the domains.

(b). 1 year after rolling. The domain boundaries are evident now only through the discontinuities of the extinction contours.

evidence indicating that the internal strain is less than in Fig. 8. Another section was prepared after the rolled sheet had stood for about one year with the result shown in Fig. 9b. The domain boundaries in this section are made visible chiefly through the discontinuities in the extinction contours rather than overall contrast between domains. Apparently the domains slowly relieve their internal strains and become less distinct as recovery proceeds at room temperature.

A possible complication in the study of thin sections in the electron microscope is the effect of rather intense electron bombardment. There are several possible ways in which the sections might be changed by bombardment. One of these is simply annealing due to heating by bombardment. However, the metal is a good conductor of heat and is in contact with the heavy brass specimen holder so that high local temperatures would not be expected as with thermal insulators or isolated particles. Another phenomenon that is quite common is the deposition of a carbonaceous layer on the areas exposed to the electron beam. This is generally due to the residual hydrocarbon atmosphere in the vacuum system and is visible to the naked eye as a black deposit. The remaining possibility is that of producing lattice defects or vacancies by collision with the incident electrons. The cross-section for this process is not known but it would be expected that for 50 KV electrons it would be quite small.

Many thin sections of aluminum have been examined in the RCA EMU instrument at moderate intensities using the biased electron gun with little evidence for any changes occurring over the normal times required for obtaining pictures. However, if the peak intensity attainable with the biased is used, quite significant changes occur as illustrated in Fig. 10. These images are taken from a sequence and show the effect of time of bombardment on the recovery domains. The loss of contrast and irreversible changes in details with time of bombardment are evident. Part of the effect is due to heating and part to deposition but in general the behavior is not understood.

An outstanding feature of the domains in cold worked, high purity aluminum has been the relatively uniform size exhibited over a great many samples prepared at room temperature. The deformations have ranged from the order of about 30% to several hundred percent with the domain size consistently in the neighborhood of 2μ. At low deformations of the order of a few percent the domains are not found. No growth or change in size of any consequence has been found after months at room temperature. The relief of internal strains seems to be the only significant change with time. A short anneal at or above the recrystallization temperature removes the domains and gives rise to new crystals which exhibit extinction contours. Observations such as this tie the domain structure quite firmly to recovery.

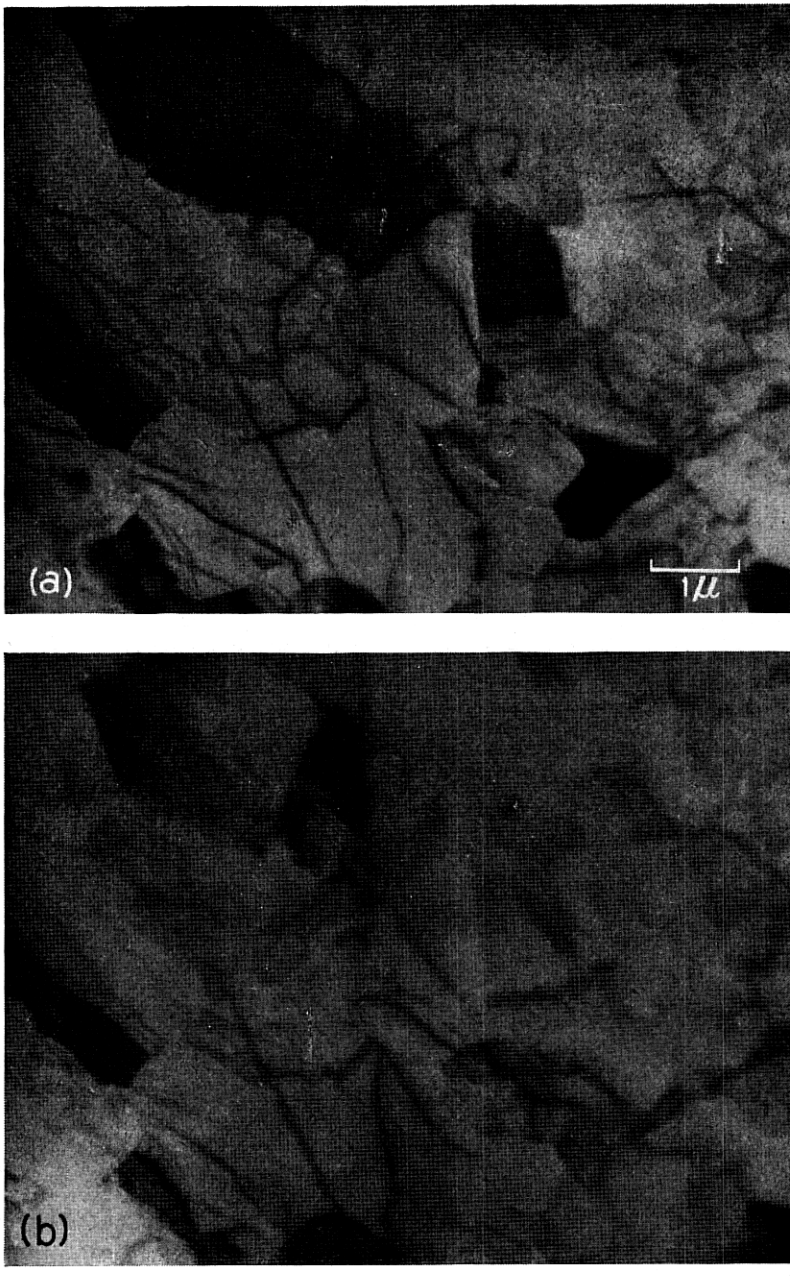

Fig. 10—Effect of intense electron bombardment (5OKV electrons) on the domain structure.
(a) 45 seconds bombardment
(b). 125 seconds bombardment

As previously pointed out, the formation of recovery domains upon cold working represents an early stage of polygonization with a much smaller size than that observed at low deformation.[10] This suggests a nucleation and growth process[11] for recovery during and following plastic deformation. Cahn[12] has published a detailed nucleation theory to account for recrystallization grain size. He considers the nuclei to be regions in the crystal with large curvature brought about by cold working. It would be expected that both the nucleation and growth rates would be effected by changes in temperature and by additions of alloying elements which reduce the rate of diffusion of dislocations. The latter was tried first by adding about 4% copper to the high purity aluminum and rolling the alloy to 0.005″ sheet. A section prepared from the rolled sheet with no anneal gave the results shown in Figure 11. It will be noted in Fig. 11a that the large, well defined domains seen in Figs. 8 and 9 are not present in the alloy. The structure is much smaller and is strung out in the direction of rolling. The electron diffraction pattern, (Fig. 11(b)) exhibits arced rings with the arcs being continuous rather than showing the discrete spots seen for the pure metal (Fig. 8b). The number of recovery domains produced in the alloy is thus much greater than in the base metal which checks with the much smaller recovery exhibited by cold worked aluminum alloys as compared to pure aluminum. It is concluded that the addition of copper has produced "knots" in the aluminum lattice which impede the rate of growth of domains.[13]

The effect of temperature is of much interest since nucleation processes generally involve a temperature dependent term of the form $e - \frac{A}{KT}$ where A is an activation energy[14] A plot of nucleation rate against temperature should yield a curve exhibiting a maximum at some temperature T_c. For $T > T_c$, only a portion of the embryos are able to exceed the critical size, the smaller ones dissociating. For $T < T_c$, the thermal diffusion rates are sufficiently low to impede embryo formation. The maximum nucleation rate is thus a balance between the diffusion rate and the number of embryos able to exceed the critical size and grow. In order to investigate the effect of temperature, high purity aluminum specimens were cold worked by pounding at −78°C (dry ice) and at −196°C (liquid nitrogen) and then allowing the specimen to warm up slowly to room temperature. It was thought that if the working was done at a temperature below that at which

[10] A. Guinier and J. Tennevin, C. R. Acad. of Sci., Paris *226*, 1530 (1948).
[11] R. D. Heidenreich, "Cold Working of Metals," page 57 (American Society for Metals, Cleveland, 1949.
[12] R. W. Cahn, *Proc. Phys. Soc. A 63*, 323 (1950).
[13] If this alloy is given a 10 min. anneal at 300°C, recovery domains very similar to Fig. 8 are obtained.
[14] D. Turnbull, *A.I.M.M.E. Gech. Pub.* #2365 (1948).

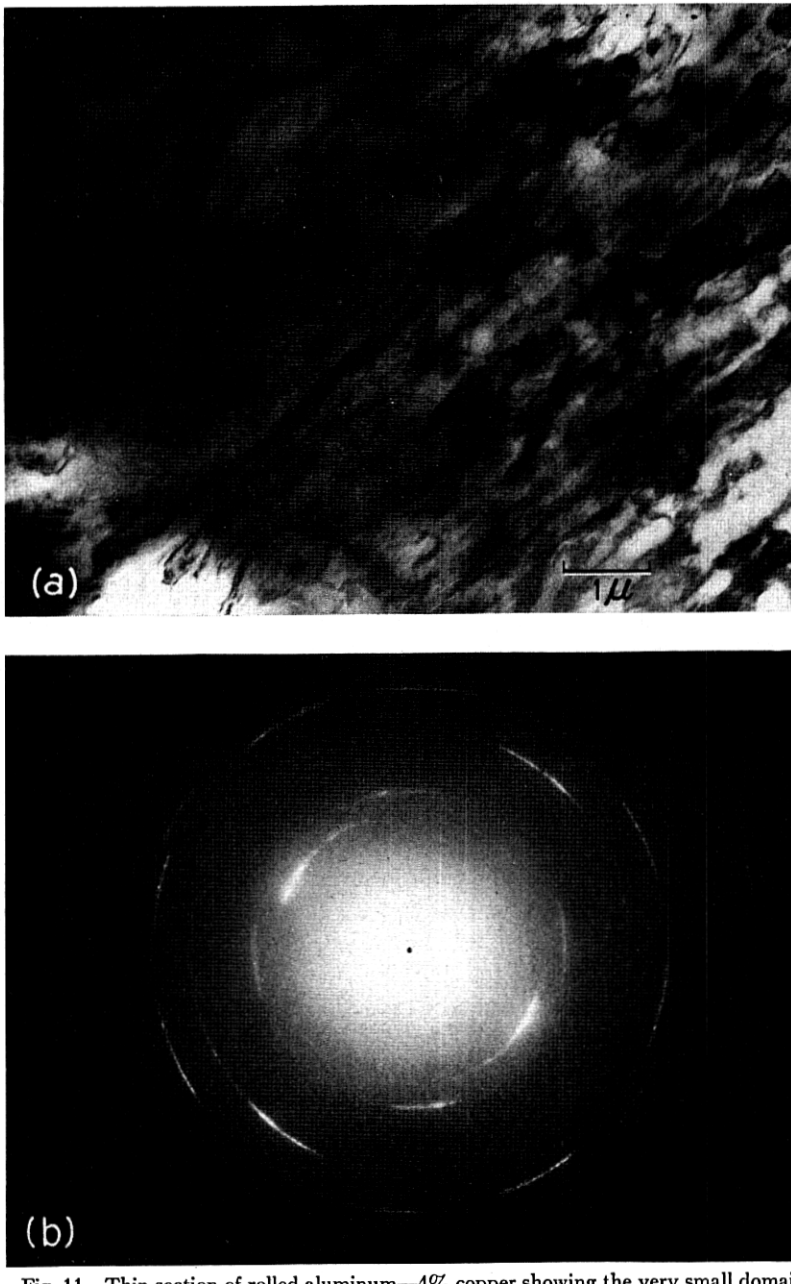

Fig. 11—Thin section of rolled aluminum—4% copper showing the very small domains. (b) is a transmission electron diffraction pattern. Compare with Fig. 8.

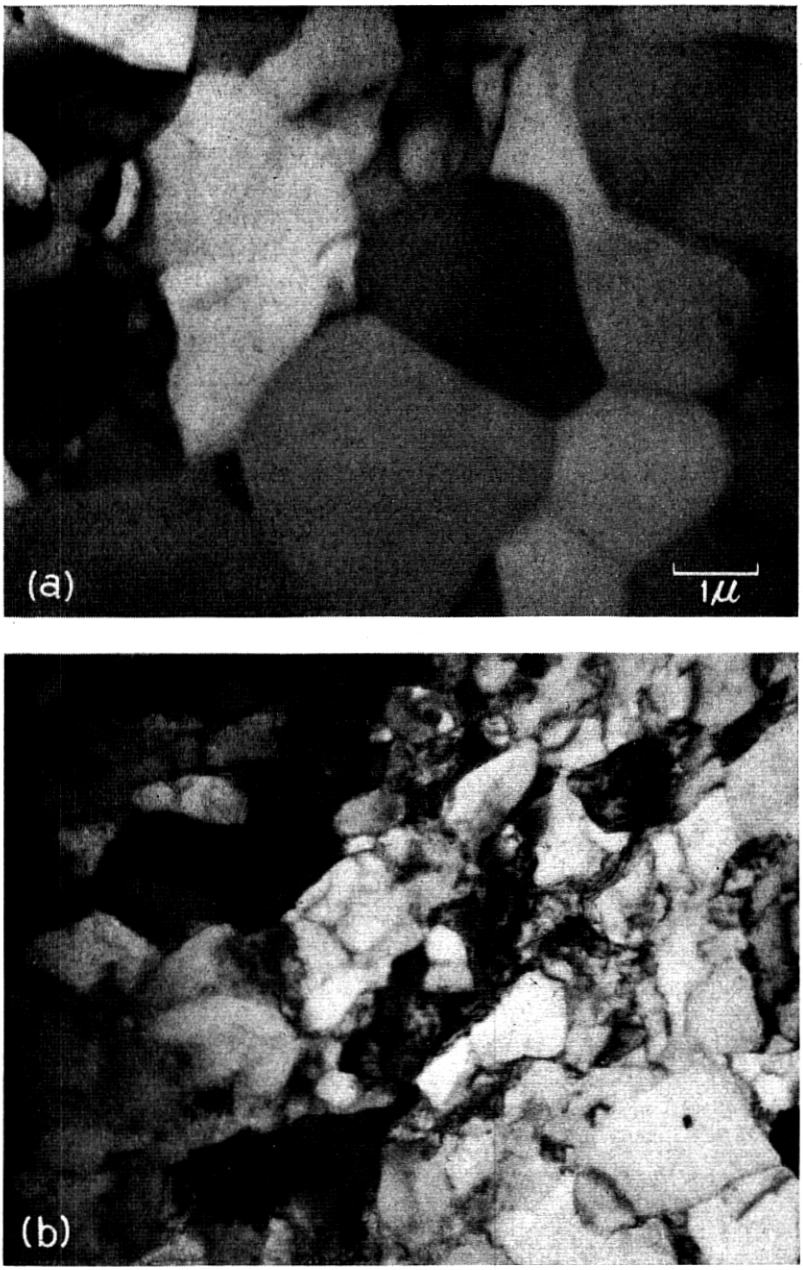

Fig. 12—Effect of temperature at which recovery proceeds on domain size in high purity aluminum.
(a). Dry ice (−78°C)
(b). Liquid nitrogen (−196°C)

the nucleation rate is a maximum, then as the specimen warmed slowly it would pass through the maximum and result in a larger number of nuclei. The time for recovery at the low temperature was varied from 15 minutes to several hours before bringing the specimen to room temperature but the results did not reflect any dependence on the time at low temperature. Even so, a primary weakness in the experiment lies in the fact that the structure could not be observed at the temperature of working. The results of cold working at −78°C and −196°C are shown in Fig. 12. Surprisingly enough, the domain size after cold working at −78°C is practically the same as at room temperature as seen in Fig. 12a. It was thought that this simply meant that the structure had reverted to the room temperature configuration until the results were obtained at −196°. The domain size resulting from the −196°C treatment is slightly less than half that obtained from the −76°C treatment, indicating that the effect of recovery temperature can be seen after bringing the specimen up to room temperature.[15] This is consistent with low temperature rolling experiments[16] on pure copper performed by W. C. Ellis and E. Greiner of Bell Telephone Laboratories in which the amount of work hardening was considerably increased over that obtained by rolling at room temperature. Thus, at present it appears that the recovery domains seen in Fig. 12 are a fair approximation to those produced at the low temperatures. More work on low temperatures is certainly justified since it appears that the recovery mechanism involves a process with a very low activation energy, at least in the case of pure aluminum.

General Remarks

The conclusions drawn from the electron images of cold worked aluminum are, in review,

(1) During and immediately following cold working of pure aluminum self-recovery takes place by the formation of recovery domains about 2μ in size.
(2) The recovery domains produced at room temperature and below at first possess sufficient internal strains to prohibit extinction contours. These strains are slowly relieved at room temperature.
(3) The addition of copper to the aluminum inhibits the growth of recovery domains resulting in a recovery domain size much smaller than for the pure metal. Thus, aluminum-copper work hardens to a far greater extent than does pure aluminum.
(4) Recovery in pure aluminum is reduced only by going to relatively

[15] The microbeam x-ray technique (reference 9) should be invaluable in checking this point since the entire experiment could be done at the low temperature.
[16] To be published.

low temperatures; i.e., of the order of that of liquid nitrogen (−196 °C).

(5) The recovery domains do not show (at least not readily) on etched surfaces. The overall rate of etching is much higher than in the annealed state, however.

(6) Deformation by simple extension does not produce the recovery domains such as seen in Fig. 8. Neither domains nor slip bands are visible.

These conclusions and observations suggest explanations for several well known phenomena in cold worked metals. One is the fact that slip lines are not visible on a surface etched *after* cold working, which has always been rather puzzling. It seems clear now that this is simply due to an immediate rearrangement giving rise to recovery so that the slip band exists as such *only during the actual deformation process*. The traces left on polished surfaces are actually only traces of the displacements that occurred during deformation and do not indicate where the energy of cold work resides when slipping has stopped but only where the energy was introduced. The energy would reside in the slip bands only if no recovery whatever took place.

Another point of interest is that of recrystallization. In one sense the recovery domains constitute recrystallization on a smaller scale than is usually meant. However, in view of the fact that the domains do not etch preferentially (probably due to internal strains) and that they disappear at the recrystallization temperature, it would seem more accurate to view the recovery domains as distinct from recrystallization. It would seem logical to consider the recovery domains as *embryos* for recrystallization. When the temperature is raised sufficiently those recovery domains which most rapidly relieve their internal strains would serve as nuclei for new grains and consume the surrounding embryos or domains. In a sense, then, it is the least strained material from which new grains spring. However, the embryo for the new grain very probably sprang from a region that was very highly strained. Between the actual slip process and final recrystallization grains there are actually two nucleation and growth processes.

The author is grateful to Mr. W. T. Read and Dr. W. Shockley for valuable criticisms and discussions of the subject matter presented in this paper.